PHYSICAL REVIEW C **108**, 054604 (2023)

Modifying the electron capture decay rate of ^{7}Be by using small fullerenes

Zhaoyang Li[1] and Tao Yang[1,2,*]
[1]*MOE Key Laboratory for Non-Equilibrium Synthesis and Modulation of Condensed Matter, School of Physics,*
Xi'an Jiaotong University, Xi'an 710049, Shaanxi, China
[2]*Xi'an Jiaotong University Suzhou Academy, Suzhou 215123, Jiangsu, China*

(Received 19 June 2023; revised 30 August 2023; accepted 12 September 2023; published 17 November 2023)

Electron capture (EC) decay of a ^{7}Be atom, the rate of which is affected by the electron density at the ^{7}Be nucleus, forms a ^{7}Li atom and emits a neutrino. Herein, we studied the EC decay rate of $^7\mathrm{Be@C}_{2n}$ ($2n = 24$, 28, 32, 36, 50), in which those fullerenes have enhanced stability relative to their near neighbors, by using *ab initio* calculations. The stable and metastable ^{7}Be atom sites and electron density at the ^{7}Be nucleus in $^7\mathrm{Be@C}_{2n}$ were calculated. Unlike $^7\mathrm{Be@C}_{60}$, the ^{7}Be nucleus sites in $^7\mathrm{Be@C}_{2n}$ ($2n = 24$, 28, 32, 36, 50) are always off center and close to the fullerene cage. Due to the bonding interaction between ^{7}Be and the fullerene cage, the electron density at the ^{7}Be nucleus in $^7\mathrm{Be@C}_{2n}$ is smaller than those of a single ^{7}Be atom and of ^{7}Be in $^7\mathrm{Be@C}_{60}$, leading to the result that the half-life of ^{7}Be in $^7\mathrm{Be@C}_{2n}$ increases. Based on equilibrium statistical thermodynamic calculations, the temperature effect on the half-life of ^{7}Be has been analyzed. In contrast to $^7\mathrm{Be@C}_{60}$, the temperature only slightly influences the half-life of ^{7}Be in $^7\mathrm{Be@C}_{2n}$ suggesting that the EC decay rate of ^{7}Be could be precisely modified by using small fullerene cages.

DOI: 10.1103/PhysRevC.108.054604

I. INTRODUCTION

Electron capture (EC) decay is a radioactive process by which a proton in the nucleus acquires an electron from atomic or molecular shell, thereby forming a neutron and emitting a neutrino [1],

$$p + e^- = n + \nu_e, \tag{1}$$

where p, e^-, n, and ν represent proton, electron, neutron, and electron neutrino. ^{7}Be has a simple electron structure ($1s^2 2s^2$), a short half-life (53.22 days) [2], a low measurement error, and 100% of the decay process is EC decay, thus it is a very suitable nuclide to study EC decay. Segrè [3] and Daudel [4] independently proposed in 1947 that the EC decay rate of radioactive matter is proportional to electron density near the nucleus, indicating that the EC decay rate of a light element like Be could be moderately altered by putting it in different chemical compounds. Since then, many experimental measurements of ^{7}Be EC decay in different chemical forms and media have been reported.

The strategies to control the EC decay rate of ^{7}Be could be simply divided into physical and chemical ways. For the chemical ways, the half-lives of ^{7}Be in those compounds were altered via chemical bonding between ^{7}Be and neighbor atoms. ^{7}Be was inserted into different metals or compounds such as Cu, Al [5], Pd, W [6], and BeO [7]. In the case of physical ways, electric field, air pressure, as well as temperature have been utilized on those ^{7}Be-containing compounds to modify the electron density near the nucleus and resulting EC decay rate [8,9]. For instance, Gholamian *et al.* revealed that the half-life of ^{7}Be in Be metal was altered approximately 0.02% by using an electric field strength of 5.14 V/Å [10]. The half-life of ^{7}Be in crystalline $\mathrm{Be(OH)_2}$ could be reduced by 1% at 400 kbar compared to that at one standard atmosphere pressure [11].

By employing a recoil process of the nuclear reactions, one ^{7}Be atom was penetrated into the C_{60} cage and endohedral fullerene $^7\mathrm{Be@C}_{60}$ was generated ($M\mathrm{@C}_{2n}$ indicates that M atom is embedded in the C_{2n} cage) [12]. The ^{7}Be EC decay rate in $^7\mathrm{Be@C}_{60}$ was enhanced by 1.1% compared to ^{7}Be metal, resulting in 52.65 and 53.25 days half-life for $^7\mathrm{Be@C}_{60}$ and ^{7}Be metal, respectively. The modification of ^{7}Be half-life in C_{60} comes from the increasing electron density at the ^{7}Be nucleus sites in $^7\mathrm{Be@C}_{60}$ due to the attractive effective potential well generated by C_{60} [13]. Meanwhile, the ^{7}Be decay rates in exohedral and endohedral C_{60} fullerene have been measured, and have different half-lives [14]. The half-life of cooled $^7\mathrm{Be@C}_{60}$ at 5 K is found to be 52.47 days, 0.34% faster than that at $T = 293$ K [12,15]. The reason why temperature could affect the EC decay rate comes from the fact that there are five stable Be nucleus sites in C_{60} with different electron densities, and temperature could influence the Boltzmann distribution of those five Be nucleus sites [16]. Other investigations found that the half-life decay time of the ^{7}Be nucleus in $^7\mathrm{Be@C}_{36}$ is longer than that of $^7\mathrm{Be@C}_{60}$ at 0 K [17,18]; however, the EC decay rate of the ^{7}Be nucleus in $^7\mathrm{Be@C}_{70}$ is similar to that in $^7\mathrm{Be@C}_{60}$ at 0 K [19]. A series of ^{7}Be compounds including several ^{7}Be-encapsulated fullerenes have been studied at 0 K by Yoshida and co-workers [20]. Very recently, Ohtsuki, Kuwahara, and Ohno experimentally measured the half-lives of ^{7}Be in endohedral fullerene $^7\mathrm{Be@C}_{70}$ at room temperature ($T = 293$ K) and at liquid helium temperature ($T = 5$ K), which are 52.49 ± 0.04 and 52.42 ± 0.04 d, respectively [21].

---

[*] taoyang1@xjtu.edu.cn

In the present study, we studied the possible Be nucleus sites, energies, stabilities, and electron structures of small endohedral fullerenes ^{7}Be@C$_{2n}$ ($2n = 24, 28, 32, 36, 50$) as well as ^{7}Be@C$_{60}$ by employing *ab initio* calculations, because, according to the empirical rules proposed by Kroto, those fullerenes C$_{2n}$ ($2n = 24, 28, 32, 36, 50, 60$) exhibit enhanced stability relative to their near neighbors [22]. The ^{7}Be EC decay rate is estimated by using electron densities at the ^{7}Be nucleus from wave-function calculations. Compared to that of ^{7}Be@C$_{60}$, the half-lives of ^{7}Be in those ^{7}Be@C$_{2n}$ are higher, above 53.6 days. More importantly, the temperature effect on the EC decay rates of ^{7}Be in those ^{7}Be@C$_{2n}$ has been studied via calculating the possible distribution of different Be nucleus sites in a given fullerene cage.

II. CALCULATION METHOD

Geometric optimizations of ^{7}Be@C$_{2n}$ ($2n = 24$, 28, 32, 36, 50) were performed in the GAUSSIAN09 package [23] by using density functional calculations. Several functionals with the Grimme's D3 [24,25] dispersion corrections, including BP86-D3 [26,27], B3LYP-D3 [28,29], PBE-D3 [30], PBE0-D3 [31], M06-2X-D3 [32], and ωB97XD [33], were employed with the basis set def2-TZVP. The PBE0-D3 function was found to be able to reproduce the experimental adiabatic ionization energy and electron affinity of C$_{60}$ well. Thus, all the calculations of geometric optimizations were performed by using PBE0-D3(BJ)/def2-TZVP [34], and subsequent calculations are based on these structures.

The program package ADF2019 [35] describes the electron wave functions by Slater-type orbitals (STOs), which is better for describing the wave functions at the nucleus than Gaussian-type orbitals (GTOs), so ADF is used for single-point energy calculation of the electron density at the ^{7}Be nuclear point. The calculations were performed with PBE0-D3(BJ)/QZ4P, which is the largest and most accurate basis set. The electron density value is the average result of a spherical space with a distance of 2.98 fm from the ^{7}Be nucleus.

Given the small size of the nucleus, the nuclear wave functions are not affected by the chemical environment, so the variation of EC decay rate, $d\lambda_{\mathrm{EC}}$, can be represented as [36]

$$d\lambda_{EC} = \left(\frac{\rho_e}{\rho_{ref}} - 1\right)\lambda_{ref}, \tag{2}$$

where λ is decay rate and ρ is electron density. Equation (2) shows that the variation in the EC decay rate is proportional to the change in the electron density at the nucleus [$\rho(0)$]. The electron density as a function of the distance from the atomic radius of ^{7}Be is calculated by MULTIWFN [37].

The radial distribution function is obtained as

$$RDF(r) = \int f(r, \Omega) r^2 d\Omega, \tag{3}$$

where r is the distance from selected center, and Ω represents the angular coordinate in the sphere layer.

TABLE I. Possible structures of ^{7}Be@C$_{2n}$ ($2n = 24$, 28, 32, 36, 50) with the spin states of singlet (S) and triplet (T). ΔE is the energy difference between the most stable structure and metastable structures. E_b is the binding energy with respect to the pristine fullerenes and ^{7}Be. The energy unit is eV. The Sym. represents new symmetry of the whole ^{7}Be@C$_{2n}$.

	ΔE	E_b	Sym.
^{7}Be@C$_{24}$ S-Iso1	0.00	1.67	S_2
^{7}Be@C$_{28}$ S-Iso1	0.29	2.67	C_{3v}
^{7}Be@C$_{28}$ T-Iso2	0.00	2.96	C_{3v}
^{7}Be@$D_3(6)-$C$_{32}$ S-Iso1	0.00	1.10	C_2
^{7}Be@$D_3(6)-$C$_{32}$ S-Iso2	0.05	1.05	C_3
^{7}Be@$D_{2d}(14)-$C$_{36}$ S-Iso1	0.00	1.51	C_s
^{7}Be@$D_{2d}(14)-$C$_{36}$ S-Iso2	0.24	1.27	C_2
^{7}Be@$D_{2d}(14)-$C$_{36}$ T-Iso3	0.12	1.39	C_1
^{7}Be@$D_3(270)-$C$_{50}$ S-Iso1	0.00	0.94	C_1
^{7}Be@$D_3(270)-$C$_{50}$ T-Iso2	0.19	0.75	C_2
^{7}Be@$D_3(270)-$C$_{50}$ T-Iso3	0.29	0.65	C_1
^{7}Be@$D_{5h}(271)-$C$_{50}$ S-Iso1	0.00	2.22	C_{2v}

As shown by Ohtsuki *et al.* [15,16], the half-life of ^{7}Be in C$_{60}$ is affected by the temperature, because temperature could influence the Boltzmann distribution of those possible Be nucleus sites. Since there are several possible Be nucleus sites in ^{7}Be@C$_{2n}$ ($2n = 24, 28, 32, 36, 50$) for a given fullerene, the temperature could also affect the possible Boltzmann distribution of those isomers and consequently the ^{7}Be half-life. To study the relative concentrations of those isomers, the relative populations of m isomers in their equilibrium mixture can be expressed as their mole fractions, w_i, using the isomeric partition functions q_i. In the terms of q_i and the ground-state energy changes $\Delta H^o_{0,i}$, the mole fractions are given by a compact formula [38]:

$$w_i = \frac{q_i \exp\left[-\Delta H^o_{0,i}/(RT)\right]}{\sum_{j=1}^{m} q_j \exp\left[-\Delta H^o_{0,j}/(RT)\right]}, \tag{4}$$

where R stands for the gas constant and T for the absolute temperature. The partition functions are to be practically constructed within the rigid-rotor and harmonic-oscillator approximation. By using this partition functions, all the entropy contributions are evaluated and the standard temperature-dependent Gibbs energies of the isomers are derived further by involving the enthalpy terms that come from the above potential energy calculations, on the basis of the principle of equilibrium statistical thermodynamics. This method has been developed and successfully employed to predict the relative concentrations of pristine fullerene [39] and endohedral fullerene isomers [40–42].

III. RESULTS AND DISCUSSION

A. Geometries and relative energies of Be@C$_{2n}$ at 0 K

Six fullerene cages including C$_{24}$, C$_{28}$, $D_3(6) -$ C$_{32}$, $D_{2d}(14) -$ C$_{36}$, $D_{5h}(271) -$ C$_{50}$ and $D_3(270) -$ C$_{50}$ were chosen, because $D_{5h}(271) -$ C$_{50}$ and $D_3(270) -$ C$_{50}$ have almost similar stability [39,43]. To confirm the spin state of ^{7}Be@C$_{2n}$, both the singlet and triplet states were examined. Table I presents the possible stable structures with relative energy lower than 0.3 eV. The binding energies E_b are higher than 0.65 eV, suggesting that ^{7}Be prefers to stay inside the

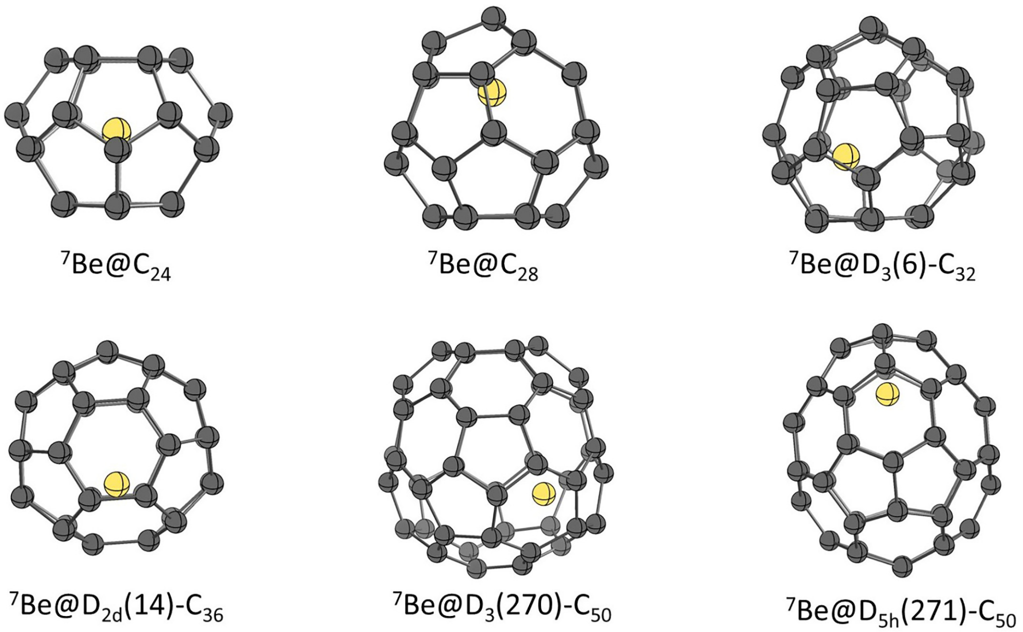

FIG. 1. Optimized structures of ^{7}Be@C$_{2n}$ ($2n = 24, 28, 32, 36, 50$).

fullerenes. Except for ^{7}Be@C$_{28}$, all the ground states are singlet.

The most stable structures of ^{7}Be@C$_{2n}$ are shown in Fig. 1, with the metastable structures of ^{7}Be@C$_{2n}$ exhibited in the Supplemental Material [44]. Unlike the results of ^{7}Be@C$_{60}$, ^{7}Be in the most stable structures of ^{7}Be@C$_{2n}$ is not located at the center of the fullerene cage, so the original symmetry of the fullerene cage is broken. For ^{7}Be $@D_3(270) - C_{50}$ and ^{7}Be $@D_{5h}(271) - C_{50}$, there are local minima with ^{7}Be is at the center of the fullerene cage; however, these structures are significantly at least 0.81 eV higher in energy than the most stable structure. The bond lengths between ^{7}Be and carbon atoms fall in a narrow range from 1.699 Å for ^{7}Be@C$_{28}$ to 1.753 Å for ^{7}Be@C$_{24}$.

B. Electron density and half-life of the ^{7}Be atom in ^{7}Be@C$_{2n}$

According to the above Eq. (2), the half-life of the ^{7}Be atom depends on the electron density at the ^{7}Be nucleus [$\rho(0)$] in ^{7}Be@C$_{2n}$. Thus, the electron densities $\rho(0)$ of the ^{7}Be atom in all the most stable ^{7}Be@C$_{2n}$ ($2n = 24$, 28, 32, 36, 50, 60) were calculated, as shown in Table II. The result for a ^{7}Be atom is also calculated for comparison. The electron density $\rho(0)$ in ^{7}Be@C$_{60}$ is higher than that of a single ^{7}Be atom, and the difference between the electron density $\rho(0)$ of the ^{7}Be atom and ^{7}Be@C$_{60}$ is 0.17%, consistent with the previously calculated value [15]. The half-life of the ^{7}Be atom in ^{7}Be@C$_{60}$ is as short as 52.470 days, suggesting that C$_{60}$ speeds up the EC decay rate. However, other ^{7}Be@C$_{2n}$ ($2n = 24$, 28, 32, 36, 50) have lower electron density $\rho(0)$ than one single ^{7}Be atom. Based on the electron density $\rho(0)$ and the half-life of ^{7}Be in ^{7}Be@C$_{60}$ at 5K, the half-lives of ^{7}Be in ^{7}Be@C$_{2n}$ ($2n = 24$, 28, 32, 36, 50) were calculated and the results are shown in Table II and Fig. 2. All those half-lives are higher than 53.6 days, 2.11% to 2.16% longer than that of a ^{7}Be atom, revealing that the EC decay rates of the ^{7}Be atom in ^{7}Be@C$_{2n}$ ($2n = 24$, 28, 32, 36, 50) have been slowed down by those small fullerenes. The above results show that EC decay rate could be modified by using different fullerene cages.

To reveal why the electron density at the Be nucleus, $\rho(0)$, changes in ^{7}Be@C$_{2n}$ ($2n = 24$, 28, 32, 36, 50), the contributions of molecular orbitals (MOs) to the electron density at the ^{7}Be nucleus point were analyzed, as shown in Table III. For all the ^{7}Be@C$_{2n}$ and for the single ^{7}Be atom, the contribution of the ^{7}Be-1s orbital to electron density $\rho(0)$ is important. However, the contribution from the Be-2s orbital is different. For the ^{7}Be atom and ^{7}Be@C$_{60}$, it is the second most important contributing orbital at about 3.7%, whereas it is the third most important contributing orbital for other ^{7}Be@C$_{2n}$ with

TABLE II. The electron density at Be nucleus $\rho(0)$ ($e^-/\alpha_{\rm B}^3$) and half-life (days) of single ^{7}Be atom and ^{7}Be in ^{7}Be@C$_{2n}$ ($2n = 24$, 28, 32, 36, 50, 60).

	Electron density at Be nucleus (e^-/α_B^3)	Half-life (days)
^{7}Be@C$_{24}$ S-Iso1	35.104	53.628
^{7}Be@C$_{28}$ T-Iso2	35.089	53.652
^{7}Be@D$_3$(6)$-$C$_{32}$ S-Iso1	35.084	53.658
^{7}Be@D$_{2d}$(14)$-$C$_{36}$ S-Iso1	35.067	53.654
^{7}Be@D$_3$(270)$-$C$_{50}$ S-Iso1	35.104	53.628
^{7}Be@D$_{5h}$(271)$-$C$_{50}$ S-Iso1	35.095	53.643
^{7}Be atom	35.844	52.522
^{7}Be@C$_{60}$	35.879	52.470[a]

[a] Experimentally measured half-life of ^{7}Be in ^{7}Be@C$_{60}$ at 5 K [15], which is taken as the reference to calculate other half-lives.

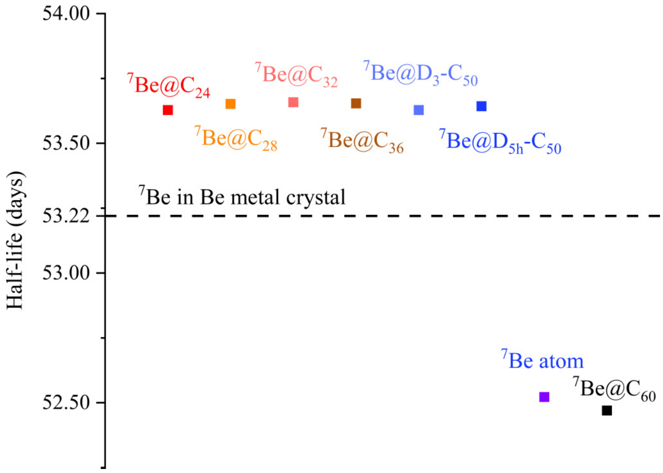

FIG. 2. The half-life of ^{7}Be in all the most stable ^{7}Be@C$_{2n}$ ($2n =$ 24, 28, 32, 36, 50). The black dotted line is the experimental value for ^{7}Be in Be metal crystal. The experimentally observed half-life (52.470 days) of ^{7}Be@C$_{60}$ is taken as the reference to calculate half-life of ^{7}Be in ^{7}Be@C$_{2n}$ ($2n = 24$, 28, 32, 36, 50).

only about $0.3-0.4\%$, thereby further affecting the electron density $\rho(0)$.

Figure 3 shows the third most important contributing molecular orbitals to the $\rho(0)$ of ^{7}Be@C$_{2n}$ ($2n = 24$, 28, 32, 36, 50) and the second most important contributing molecular orbitals to the $\rho(0)$ of ^{7}Be@C$_{60}$. Those molecular orbitals are hybridized orbitals from ^{7}Be -2s and the p orbitals of carbon atoms in ^{7}Be@C$_{2n}$ ($2n = 24$, 28, 32, 36, 50). In contrast, the ^{7}Be -2s in ^{7}Be@C$_{60}$ maintains its atomic character. These results indicate that the ^{7}Be -2s in ^{7}Be@C$_{2n}$ ($2n = 24$, 28, 32, 36, 50) contribute less to the electron density at the nuclear point than in ^{7}Be@C$_{60}$.

TABLE III. The contributions of the molecular orbitals which is mainly from Be $-$ 1s and Be $-$ 2s atomic orbitals to the electron density at the ^{7}Be nucleus point in the most stable structures of ^{7}Be@C$_{2n}$.

^{7}Be@C$_{24}$		^{7}Be@C$_{28}$	
MO	Contribution	MO	Contribution
HOMO-49	98.25%	HOMO-58	98.27%
HOMO-48	0.43%	HOMO-57	0.40%
^{7}Be @D$_3$(6) $-$ C$_{32}$		^{7}Be @D$_{2d}$(14) $-$ C$_{36}$	
MO	Contribution	MO	Contribution
HOMO-65	98.45%	HOMO-73	98.63%
HOMO-64	0.32%	HOMO-72	0.36%
^{7}Be @D_3(270) $-$ C$_{50}$		^{7}Be @D_{5h}(271) $-$ C$_{50}$	
MO	Contribution	MO	Contribution
HOMO-101	98.46%	HOMO-101	98.41%
HOMO-100	0.37%	HOMO-100	0.40%
^{7}Be@C$_{60}$		^{7}Be atom	
MO	Contribution	MO	Contribution
HOMO-121	96.17%	HOMO-1	96.31%
HOMO	3.76%	HOMO	3.69%

Furthermore, the electron density as a function of the distance from the atomic radius of ^{7}Be was also be investigated. The radial electron density is calculated by integrating the radial wave function to obtain the value of electrons, and dividing the value by the corresponding volume. Therefore, the integration accuracy will affect the results, especially the results near the nuclear point. For this reason, the electron density of ^{7}Be atoms with 0.0028 Å $\leqslant r \leqslant 0.3000$ Å is shown in Fig. 4. As in most cases, the electron density decays rapidly as the distance increases. The maximum electron density for ^{7}Be@C$_{2n}$ is different, but the change trend is very similar. Taking ^{7}Be@C$_{24}$ as an example, electron density rapidly decays to half of the maximum value at 0.0683 Å, while for a single ^{7}Be atom half of the maximum value of the electron density appears at the distance of 0.0688 Å.

C. The temperature effect on the half-life of ^{7}Be in ^{7}Be@C$_{2n}$

Morisato *et al.* found that because the temperature would affect the Boltzmann distribution of the five stable Be nucleus sites in C$_{60}$, which possesses different electron density at the ^{7}Be nucleus, the half-life of ^{7}Be in C$_{60}$ will be influenced by the temperature [16]. The calculated results for ^{7}Be@C$_{60}$ revealed that, compared with the half-life at the 0 K, the half-life at room temperature increases by 0.33%, in good agreement with the experimentally measured result (0.34%). Here, we also study the temperature effect on the half-life for ^{7}Be@C$_{2n}$ ($2n = 28$, 32, 36, 50) by calculating the Boltzmann distribution of a given ^{7}Be@C$_{2n}$ with different ^{7}Be nucleus sites based on the equilibrium statistical thermodynamic method. Except for ^{7}Be@C$_{24}$ which has only one ^{7}Be nucleus site, we calculated all the other ^{7}Be@C$_{2n}$ from 0 to 1000 K. The ^{7}Be @$D_3(6) - C_{32}$ result is shown in Fig. 5 with the other results shown in the Supplemental Material (see [44] for Figs. S2–S4). As the temperature increases, the concentration of ^{7}Be @$D_3(6) - C_{32}$/S $-$ 1 decreases while ^{7}Be @$D_3(6) - C_{32}$/S $-$ 2 increases. For example, at 1000 K the relative concentration of ^{7}Be @$D_3(6) - C_{32}$/S $-$ 1 is 75.99% while that of ^{7}Be @$D_3(6) - C_{32}$/S $-$ 2 is 24.01%, leading to the result that the half-life of ^{7}Be @$D_3(6) - C_{32}$ decreases by 0.005%. Although the relative concentration of different isomers changes evidently for a given ^{7}Be@C$_{2n}$, the half-life of the ^{7}Be atom changes slightly, as the temperature increases. This result is different from that of ^{7}Be@C$_{60}$, for which the half-life of the ^{7}Be atom changes about 0.34%. For ^{7}Be@C$_{60}$, when the ^{7}Be is at the center of the C$_{60}$ cage, it is the most stable structure and has higher $\rho(0)$ than the other four structures where the ^{7}Be atom is attached to the fullerene cage. As the temperature increases, the relative concentration of those off-center isomers increases and half-life increases moderately. For ^{7}Be@C$_{2n}$ ($2n = 28$, 32, 36, 50), the ^{7}Be is always off center and attached to the fullerene cage. The electron densities at the ^{7}Be nucleus of those sites are quite similar, thus the half-lives of ^{7}Be atoms in ^{7}Be@C$_{2n}$ are quite stable.

Notably, Ohtsuki *et al.* proposed recently that the electron-phonon couplings may play a role in affecting the EC decay

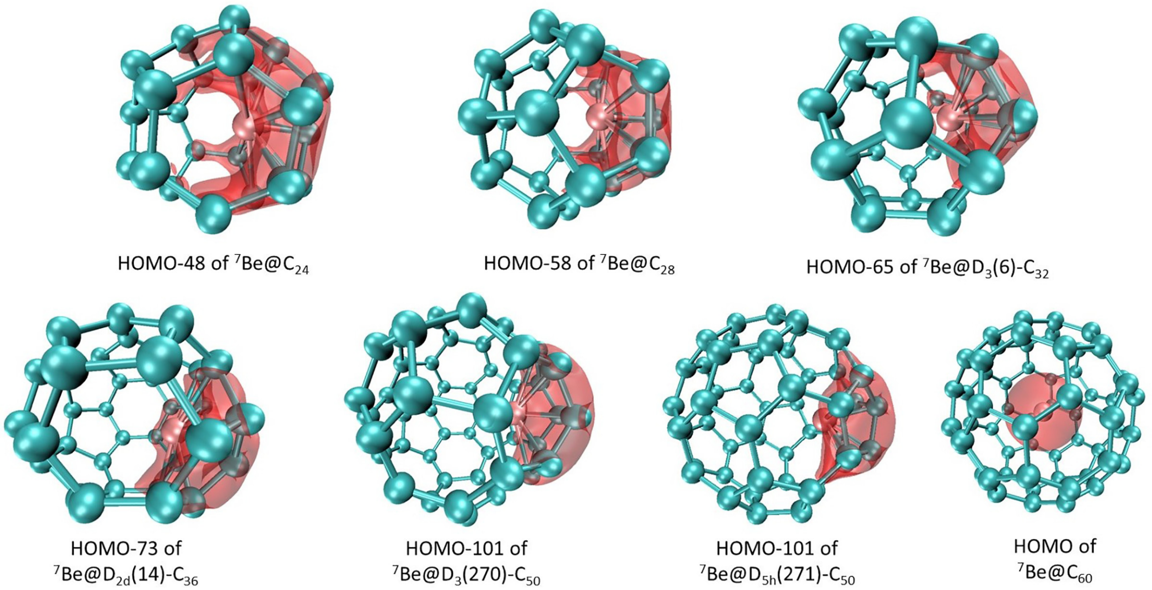

FIG. 3. The Be − 2*s*-atomic-orbital-involved molecular orbitals contributed to the electron density at the ^{7}Be nuclear point (isovalue = 0.05).

rate of ^{7}Be in ^{7}Be@C$_{60}$ and ^{7}Be@C$_{70}$ and further influence the correlation between temperature and half-life [21]. Those small endohedral fullerenes ^{7}Be@C$_{2n}$ ($2n = 24$, 28, 32, 36, 50) probably exhibit larger electron-phonon couplings than ^{7}Be@C$_{60}$ and ^{7}Be@C$_{70}$, [45,46]; however, the electron-phonon couplings effect on EC decay rate still needs further experimental and theoretical investigations.

IV. CONCLUSIONS

The most stable and metastable ^{7}Be nucleus sites in C$_{2n}$ ($2n = 24$, 28, 32, 36, 50) have been investigated by using *ab initio* calculations. The electron density at the ^{7}Be nucleus of ^{7}Be@C$_{2n}$ have been analyzed, with results suggesting that the ^{7}Be -2*s* orbital is affected by the fullerene cage, resulting in charge transfer from ^{7}Be to C$_{2n}$. The electron density at the ^{7}Be nuclear point for ^{7}Be@C$_{2n}$ ($2n = 24$, 28, 32, 36, 50) is lower than that for ^{7}Be@C$_{60}$, leading to the result that the half-life of the ^{7}Be atom in ^{7}Be@C$_{2n}$ is higher than 53.6 days, longer than that of a single ^{7}Be atom and of ^{7}Be in ^{7}Be@C$_{60}$. The temperature affects the relative concentrations of ^{7}Be@C$_{2n}$ with different ^{7}Be nucleus sites but does not change the statistical average of ^{7}Be half-life obviously,

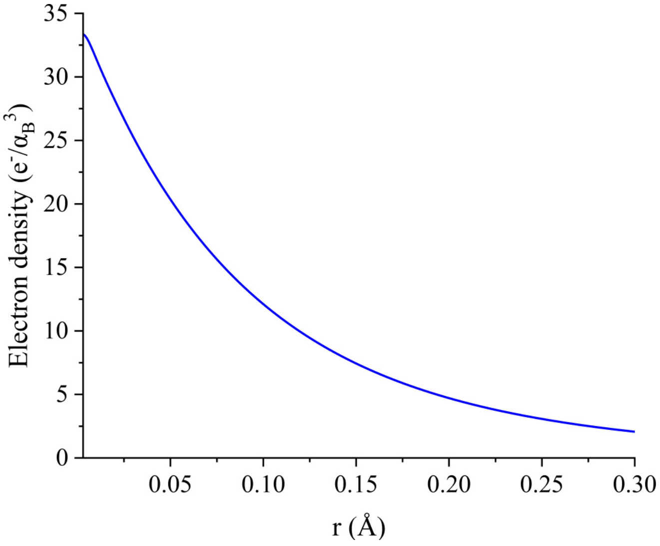

FIG. 4. The electron density as a function of the distance from the atomic radius of ^{7}Be.

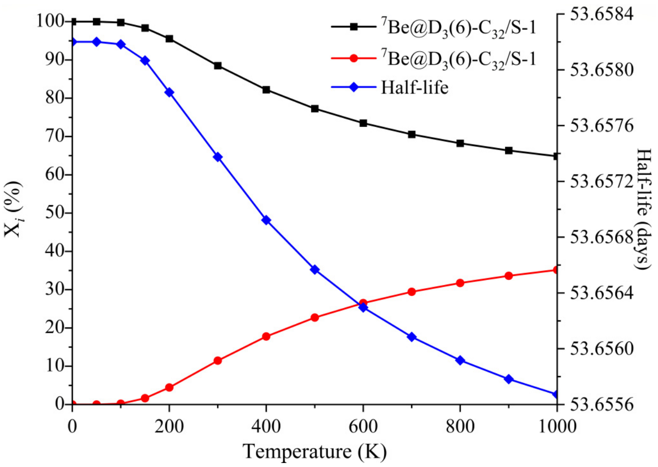

FIG. 5. Relative concentrations X_i (%) of two ^{7}Be @$D_3(6) - C_{32}$ isomers and the total half-life of ^{7}Be in ^{7}Be @$D_3(6) - C_{32}$ as the temperature increases.

because the half-lives of ^{7}Be atoms at different sites are similar. Those results reveal that the EC decay rate of ^{7}Be could be precisely modified by using those small fullerenes while not being affected by the temperature.

ACKNOWLEDGMENTS

The authors gratefully acknowledge financial support from the National Natural Science Foundation of China (Grants No. 12274337 and No. 22003048) and the Natural Science Foundation of Jiangsu Province for Youth (BK20200247).

[1] L. W. Alvarez, Phys. Rev. **52**, 134 (1937).
[2] F. G. Kondev, M. Wang, W. J. Huang, S. Naimi, and G. Audi, Chin. Phys. C **45**, 030001 (2021).
[3] E. Segre, Phys. Rev. **71**, 274 (1947).
[4] R. Bouchez, R. Daudel, P. Daudel, and R. Muxart, J. Phys. Radium. **8**, 336 (1947).
[5] Y. Nir-El, G. Haquin, Z. Yungreiss, M. Hass, G. Goldring, S. K. Chamoli, B. S. N. Singh, S. Lakshmi, U. Köster, N. Champault, A. Dorsival, G. Georgiev, V. N. Fedoseyev, B. A. Marsh, D. Schumann, G. Heidenreich, and S. Teichmann, Phys. Rev. C **75**, 012801(R) (2007).
[6] B. N. Limata, Z. Fülöp, D. Schürmann, N. De Cesare, A. D’Onofrio, A. Esposito, L. Gialanella, G. Gyürky, G. Imbriani, F. Raiola, V. Roca, D. Rogalla, C. Rolfs, M. Romano, E. Somorjai, F. Strieder, and F. Terrasi, Eur. Phys. J. A. **27**, 193 (2006).
[7] C.-A. Huh, Earth Planet. Sci. Lett. **171**, 325 (1999).
[8] A. V. Bibikov, A. V. Avdeenkov, I. V. Bodrenko, A. V. Nikolaev, and E. V. Tkalya, Phys. Rev. C **88**, 034608 (2013).
[9] A. Ray, A. K. Sikdar, P. Das, S. Pathak, and J. Datta, Phys. Rev. C **101**, 035801 (2020).
[10] F. Gholamian, M. M. Firoozabadi, and R. Sarhaddi, Chin. Phys. C **45**, 074103 (2021).
[11] L.-G. Liu and C.-A. Huh, Earth Planet. Sci. Lett. **180**, 163 (2000).
[12] T. Ohtsuki, H. Yuki, M. Muto, J. Kasagi, and K. Ohno, Phys. Rev. Lett. **93**, 112501 (2004).
[13] E. V. Tkalya, A. V. Bibikov, and I. V. Bodrenko, Phys. Rev. C **81**, 024610 (2010).
[14] A. Ray *et al.*, Phys. Rev. C **73**, 034323 (2006).
[15] T. Ohtsuki, K. Ohno, T. Morisato, T. Mitsugashira, K. Hirose, H. Yuki, and J. Kasagi, Phys. Rev. Lett. **98**, 252501 (2007).
[16] T. Morisato, K. Ohno, T. Ohtsuki, K. Hirose, M. Sluiter, and Y. Kawazoe, Phys. Rev. B **78**, 125416 (2008).
[17] E. V. Tkalya, A. V. Avdeenkov, A. V. Bibikov, I. V. Bodrenko, and A. V. Nikolaev, Phys. Rev. C **86**, 014608 (2012).
[18] F. Gholamian, M. M. Firoozabadi, and H. Raissi, Phys. Rev. C **102**, 014606 (2020).
[19] A. V. Bibikov, A. V. Nikolaev, and E. V. Tkalya, Phys. Rev. C **100**, 064603 (2019).
[20] A. Yoshida, M. Abe, and M. Hada, J. Phys. Chem. A **125**, 6356 (2021).
[21] T. Ohtsuki, R. Kuwahara, and K. Ohno, Phys. Rev. C **108**, L011301 (2023).
[22] H. W. Kroto, Nature (London) **329**, 529 (1987).
[23] M. J. Frisch *et al.*, *Gaussian 09, Revision E.01* (Gaussian,Wallingford, CT (2013).
[24] S. Grimme, S. Ehrlich, and L. Goerigk, J. Comput. Chem. **32**, 1456 (2011).
[25] S. Grimme, J. Antony, S. Ehrlich, and H. Krieg, J. Chem. Phys. **132**, 154104 (2010).
[26] J. P. Perdew, Phys. Rev. B: Condens. Matter. **33**, 8822 (1986).
[27] A. D. Becke, Phys. Rev. A **38**, 3098 (1988).
[28] A. D. Becke, J. Chem. Phys. **98**, 5648 (1993).
[29] P. J. Stephens, F. J. Devlin, C. F. Chabalowski, and M. J. Frisch, J. Phys. Chem. **98**, 11623 (1994).
[30] J. P. Perdew, K. Burke, and M. Ernzerhof, Phys. Rev. Lett. **77**, 3865 (1996).
[31] C. Adamo and V. Barone, J. Chem. Phys. **110**, 6158 (1999).
[32] Y. Zhao and D. G. Truhlar, Theor. Chem. Acc. **120**, 215 (2007).
[33] J. D. Chai and M. Head-Gordon, Phys. Chem. Chem. Phys. **10**, 6615 (2008).
[34] R. Gulde, P. Pollak, and F. Weigend, J. Chem. Theory. Comput. **8**, 4062 (2012).
[35] E. J. Baerends *et al.*, *ADF 2019, SCM, Theoretical Chemistry* (Vrije Universiteit, Amsterdam, 2019).
[36] M. S. T. Bukowinski, Geophys. Res. Lett. **6**, 697 (1979).
[37] F. Tian Lu, J. Comput. Chem. **33**, 580 (2012).
[38] Z. Slanina, X. Zhao, P. Deota, and E. Osawa, in *Fullerenes: Chemistry, Physics, and Technology*, edited by K. M. Kadish and R. S. Ruoff (John Wiley & Sons, New York, 2000), Chap. 6, p. 283.
[39] X. Zhao, J. Phys. Chem. B **109**, 5267 (2005).
[40] T. Yang, X. Zhao, and S. Nagase, Phys. Chem. Chem. Phys. **13**, 5034 (2011).
[41] T. Yang, X. Zhao, S.-T. Li, and S. Nagase, Inorg. Chem. **51**, 11223 (2012).
[42] T. Yang, X. Zhao, and S. Nagase, Chem.-Eur. J. **19**, 2649 (2013).
[43] S.-Y. Xie, F. Gao, X. Lu, R.-B. Huang, C.-R. Wang, X. Zhang, M.-L. Liu, S.-L. Deng, and L.-S. Zheng, Science **304**, 699 (2004).
[44] See Supplemental Material at http://link.aps.org/supplemental/10.1103/PhysRevC.108.054604 for Fig. S1.
[45] M. Côté, J. C. Grossman, M. L. Cohen, and S. G. Louie, Phys. Rev. Lett. **81**, 697 (1998).
[46] D. Provasi, N. Breda, R. A. Broglia, G. Colò, H. E. Roman, and G. Onida, Phys. Rev. B **61**, 7775 (2000).